[SLAC-PUB-8790]
March 2001

INTRAFIBRILLAR MINERAL MAY BE ABSENT IN DENTINOGENESIS IMPERFECTA TYPE II (DI-II)*

J. H. Kinney, T. M. Breunig, G. W. Marshall, S. J. Marshall
Department of Preventive and Restorative Dental Sciences, University of California, San Francisco, San Francisco, CA 94143-0758

J. A. Pople
Stanford Synchrotron Radiation Laboratory, Stanford Linear Accelerator Center, Stanford University, Stanford, CA 94309

C. H. Driessen
Department of Restorative Dentistry, University of Pretoria, Pretoria, South Africa

Abstract

High-resolution synchrotron radiation computed tomography (SRCT) and small angle x-ray scattering (SAXS) were performed on normal and dentinogenesis imperfecta type II (DI-II) teeth. Three normal and three DI-II human third molars were used in this study. The normal molars were unerupted and had intact enamel; donors were female and ranged in age from 18-21y. The DI-II specimens, which were also unerupted with intact enamel, came from a single female donor age 20y. SRCT showed that the mineral concentration was 33% lower on average in the DI-II dentin with respect to normal dentin. The SAXS spectra from normal dentin exhibited low-angle diffraction peaks at harmonics of 67.6 nm, consistent with nucleation and growth of the apatite phase within gaps in the collagen fibrils (intrafibrillar mineralization). In contrast, the low-angle peaks were almost nonexistent in the DI-II dentin. Crystallite thickness was independent of location in both DI-II and normal dentin, although the crystallites were significantly thicker in DI-II dentin (6.8 nm (s.d. = 0.5) vs 5.1 nm (s.d. = 0.6)). The shape factor of the crystallites, as determined by SAXS, showed a continuous progression in normal dentin from roughly one-dimensional (needle-like) near the pulp to two-dimensional (plate-like) near the dentin-enamel junction. The crystallites in DI-II dentin, on the other hand, remained needle-like throughout. The above observations are consistent with an absence of intrafibrillar mineral in DI-II dentin.

Submitted to Journal of Dental Research

* Work supported by Department of Energy contract DE-AC03-76SF00515

INTRODUCTION

Dentinogenesis imperfecta type II (DI-II) is a heritable autosomal dominant disease characterized by defects in dentin microstructure and mineralization. Unlike the form of dentinogenesis (type I) that is linked with osteogenesis imperfecta, DI-II is not believed to be associated with any known defects in collagen structure. Instead, the disease has been identified with a defect in chromosome 4 in the region 4q 12-21, implying that non-collagenous proteins are involved in the disorder (Aplin *et al.*, 1999; MacDougall *et al.*, 1996). It has been suggested that dentin matrix protein 2 (DMP2) is involved in DI-II (Thotakura *et al.*, 2000), although the involvement of other proteins has not been ruled out.

The microstructure of dentin in DI-II is altered from that of normal dentin. DI-II dentin has fewer tubules, rendering it transparent (Levin *et al.*, 1983). Those tubules that are present lack the regular organization of those in normal dentin (Siar, 1986). Furthermore, there is near total obliteration of the pulp chamber (Piattelli, 1992). However, the chief characteristic of DI-II dentin with the greatest mechanical implications is the lower mineral concentration as compared with normal dentin (Takagi *et al.*, 1983). The reduced mineralization leads to high wear rates that can cause premature failure of the teeth (Waltimo *et al.*, 1995).

In an early study of the microstructure of dentin in DI-II, it was observed that mineral crystallites appeared to form only on the exterior of the collagen fibrils (extrafibrillar mineralization), and not within the gap zones within the fibrils (intrafibrillar mineralization) (Herold, 1972). A follow up study by different investigators noted the presence of rod-shaped crystallites exterior to the collagen fibrils; intrafibrillar mineralization was not apparent in the micrographs (Kerebel *et al.*, 1981). If intrafibrillar mineralization is indeed absent in this disease, DI-II teeth would provide a unique opportunity to study the importance of intrafibrillar mineralization on the biomechanical, etching, and bonding properties of dentin. Apparently, no one has followed up or corroborated this observation.

For this study, we have used the techniques of high-resolution synchrotron radiation tomography (SRCT) and small angle x-ray scattering (SAXS) to examine the nature of the mineralization defects seen in DI-II. The SRCT quantified the mineral density distribution in the dentin, and the SAXS was used to determine the crystallite shape and thickness as a function of location within the dentin. This information was used to test the hypothesis that intrafibrillar mineralization is inhibited in DI-II.

MATERIALS AND METHODS

Specimen Preparation

Three unerupted and intact human third molars were obtained from the Core UCSF Dental Hard Tissue Specimen Core. The donors were female, and ranged in age from 18-21 years old. Immediately after extraction, the teeth were sterilized with gamma irradiation and stored intact in deionized water and thymol at 4^{o} C. The DI-II specimens came from a single female donor age 20 years with no clinical evidence of osteogenesis imperfecta (OI), although absence of OI was not entirely ruled out. These teeth were also unerupted, and the enamel was largely intact.

Synchrotron Radiation Computed Tomography (SRCT)

Prior to performing the small angle scattering studies, the teeth were imaged with SRCT. SRCT provided a noninvasive quantitative mapping of the mineral concentration in three-dimensions (Kinney *et al.*, 1994). The teeth were imaged in deionized water at the SRCT beam line 10-2 at Stanford Synchrotron Radiation Laboratory. The x-ray energy was 25.0 keV; image resolution was 17 micrometers.

The image data were reconstructed into three-dimensional mappings of the x-ray opacity with Fourier-filtered back projection. The resulting opacity data were then recombined into cubic volume elements that were 34-μm on edge to reduce the statistical noise in the data. The x-ray opacities were converted into mineral concentrations with the relation (Kinney *et al.*, 1994):

$$V_m = \frac{(\alpha_{ct} - \alpha_o)}{(\alpha_m - \alpha_o)}$$

In the above equation, α_{ct} was the measured x-ray opacity, and α_m and α_o were the opacities of the pure mineral and organic phases, respectively. The magnitude of α_o (0.44 cm^{-1}) was determined from SRCT measurements at 25 keV of EDTA-demineralized dentin matrix, and α_m (9.99 cm^{-1}) was calculated for the carbonated apatite mineral found in dentin assuming a density for the mineral crystallites of 3.0 g/cc (Kinney *et al.*, 2000a).

Small Angle X-ray Scattering (SAXS)

Within minutes after SRCT, coronal sections (250 micrometers thick) were prepared with a slow-speed diamond saw (Isomet; Buehler, Lake Bluff, IL). As water storage can alter dentin mineralization, the sections were mounted immediately after cutting and while still wet to a mechanized specimen holder and scanned by SAXS. The small angle synchrotron beamline was in close proximity to the SRCT beamline, so the time from sectioning to completion of scanning was only a few hours.

Small angle x-ray scattering was performed on beam line 1-4 at the Stanford Synchrotron Radiation Laboratory. The synchrotron radiation from a bending magnet was focused in the vertical axis by applying a small curvature to a reflecting mirror in the optical train. The beam was made monochromatic at 0.149 nm by using the {111} reflection from a silicon single crystal. Horizontal focus was obtained by using a bent silicon single crystal. Small tungsten apertures were used to collimate the beam size to 0.3 mm vertical by 0.35 mm horizontal at the specimen. For normal dentin, the x-ray beam was scanned across the specimens from the pulp to the dentin-enamel junction (DEJ) in 0.5 mm steps; for DI-II dentin, where the pulp was not apparent, the scanning direction was from the DEJ inwards. The SAXS data from each location was collected on two-dimensional imaging plate detectors (BAS-IIIs) and analyzed by methods described in greater detail in the appendix.

Crystallite shape was inferred from the logarithmic dependence of the scattering intensity with respect to the wave vector, *q*, which defined the angular dependence of the scattering with respect to the incident x-ray path (Fratzl *et al.*, 1991). Though the word shape is frequently used when describing this logarithmic dependence, this term is somewhat a misnomer as there are no unique solutions to the inverse problem of defining shape directly from the scattering profiles. It is perhaps more appropriate to consider the shape factor as providing a dimensionality, D. For D=1, the particle is roughly one-

dimensional (i.e., length), and for D=2, the particle is two-dimensional (i.e., area). Based in part on electron microscopy and the standard model of heterogeneous mineral nucleation in the collagen gaps, it has been customary to refer to the one-dimensional scattering behavior as arising from needle-like shapes, and the two-dimensional scattering behavior as arising from plate-like crystals (Fratzl *et al.*, 1992). We adopted this nomenclature for the present study with the caveat that actual shapes of the crystallites might be considerably distorted from this definition.

The surface to volume ratio of the mineral crystallites, S/V, was determined from the Porod constant, which was determined by curve fitting the q^{-4} dependence of the scattering intensity at large q (Guinier and Fournet, 1955). The data were prepared as Kratky plots and the total scattering yield was calculated. Using the total scattering yield and the Porod constant, the thickness of the crystallites, τ, was estimated from the stereological relationship $\tau = V/2S$.

RESULTS

Histology of the DI-II sections was consistent with prior studies: a virtual absence of aligned tubules, transparency, and occasional large fissures or canals (Wright and Gantt, 1985). One noteworthy finding that may have escaped prior notice was that, with drying, the DI-II specimens buckled. Buckling was reversible with rehydration. This buckling deformation was not apparent in the specimens of normal dentin.

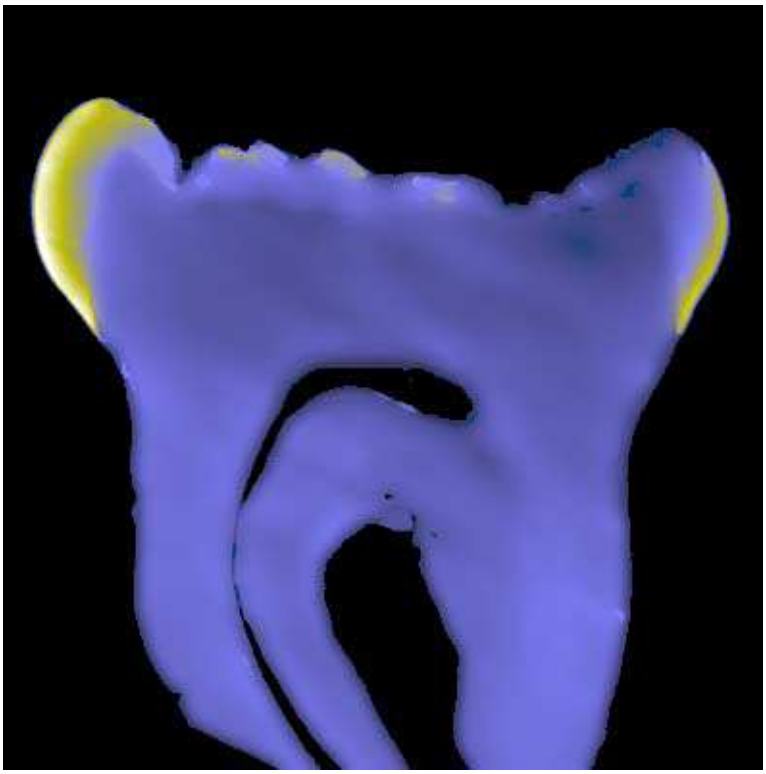

Figure 1: A sagittal section taken from a three-dimensional tomography image of a representative DI-II tooth. The image grayscale is proportional to the mineral density: the lighter region is the enamel, and the uniform gray region is the dentin. The occlusal enamel surface was not fully mineralized, and the tooth was malformed. Of particular notice was the near total obliteration of the pulp. The resolution is 34 micrometers. The dashed region corresponds to the specimen used in SAXS.

A sagittal section from a three-dimensional tomogram of a representative DI-II molar is displayed at 34-micrometer resolution in Figure 1. The image brightness (grayscale) is proportional to the mineral concentration: the lightest shading is the highly mineralized enamel, and the gray matter, which forms the bulk of the tooth, is the less mineralized dentin. The obliteration of the pulp chamber was evident in this image, as was malformation, or degradation, of the occlusal enamel. Also shown, by dashed line, is the location of the coronal section used in the SAXS study.

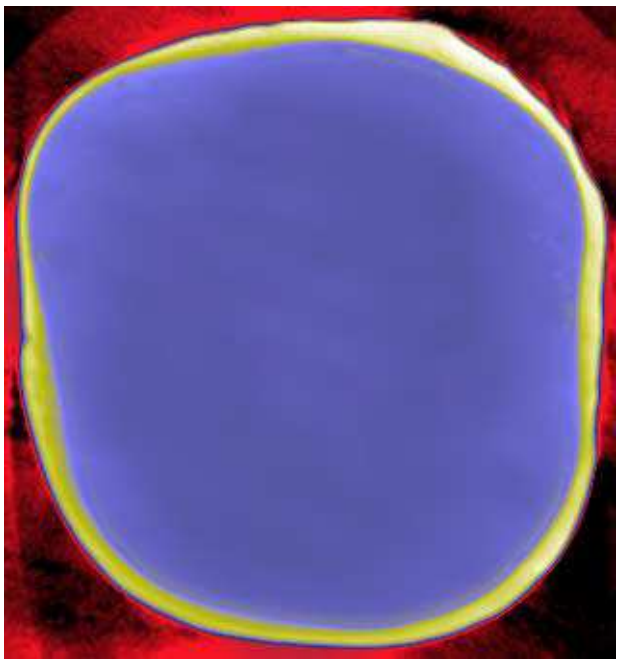

Figure 2: An occlusal section of dentin corresponding to the specimen prepared for small angle x-ray scattering. The enamel completely girdles the section. The squares correspond to the approximate beam positions where small angle x-ray scattering patterns were obtained. Resolution is 34 micrometers.

A coronal section of DI-II dentin, typical of the sections used in the SAXS studies, is shown in Figure 2. The squares correspond to the approximate locations of the SAXS measurements. This section, only slightly superior in position to the cervical margin, was notable for the absence of the pulp chamber. This was typical of all of the DI-II teeth.

The mean mineral concentration in the normal dentin, as measured by SRCT, was 39.4 percent by volume (standard deviation = 1.2). In contrast, the mean mineral concentration in the DI-II dentin was 26.5 percent by volume (standard deviation = 1.9). This difference (32.8% of the value) was highly significant ($p<0.001$). The frequency distributions of the mineral concentration for representative specimens of DI-II and normal dentin are charted in Figure 3.

Small angle scattering patterns for normal (solid line) and DI-II (dashed line) dentin are graphed in Figure 4. Characteristic of SAXS patterns for normal dentin were peaks associated with harmonics of the 67.6 nm periodic spacing of mineral-filled gap zones within the collagen fibrils. There was only the slightest evidence for diffraction in

the DI-II teeth, and the small peak that was observed was shifted, corresponding to a fundamental spacing of 63 nm.

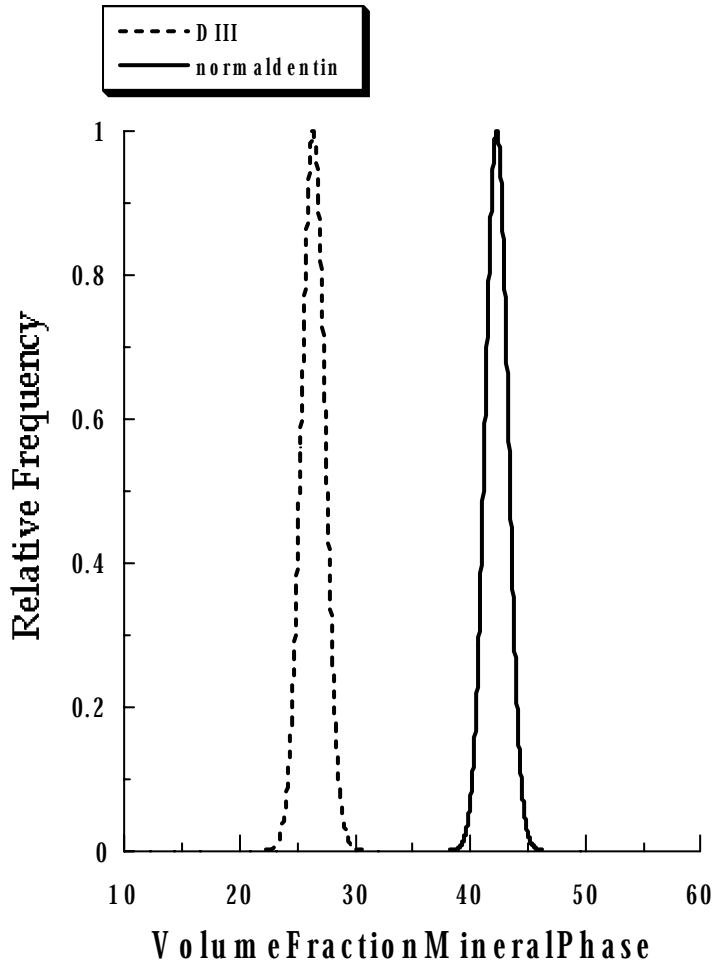

Figure 3: The frequency distributions of the mineral concentration in the middle dentin for representative specimens of DI-II and normal dentin normalized to the peak maxima. The mineral concentration in DI-II was 33% less, on average, than that in normal dentin. There was no overlap in the distributions.

In normal dentin, the shape factor varied continuously from roughly needle-like near the pulp (D=1.3) to plate-like near the DEJ (2.0). In contrast, the shape factor in DI-II dentin was uncorrelated with position; all crystallites were needle-like (D=1.43 s.d. = 0.04). In both normal and DI-II dentin, the mean crystallite thickness was invariant with location. However, the crystallite thickness in DI-II dentin (6.8nm: s.d. = 0.5) was significantly ($p<0.01$) greater than found in normal dentin (5.1nm: s.d. = 0.6).

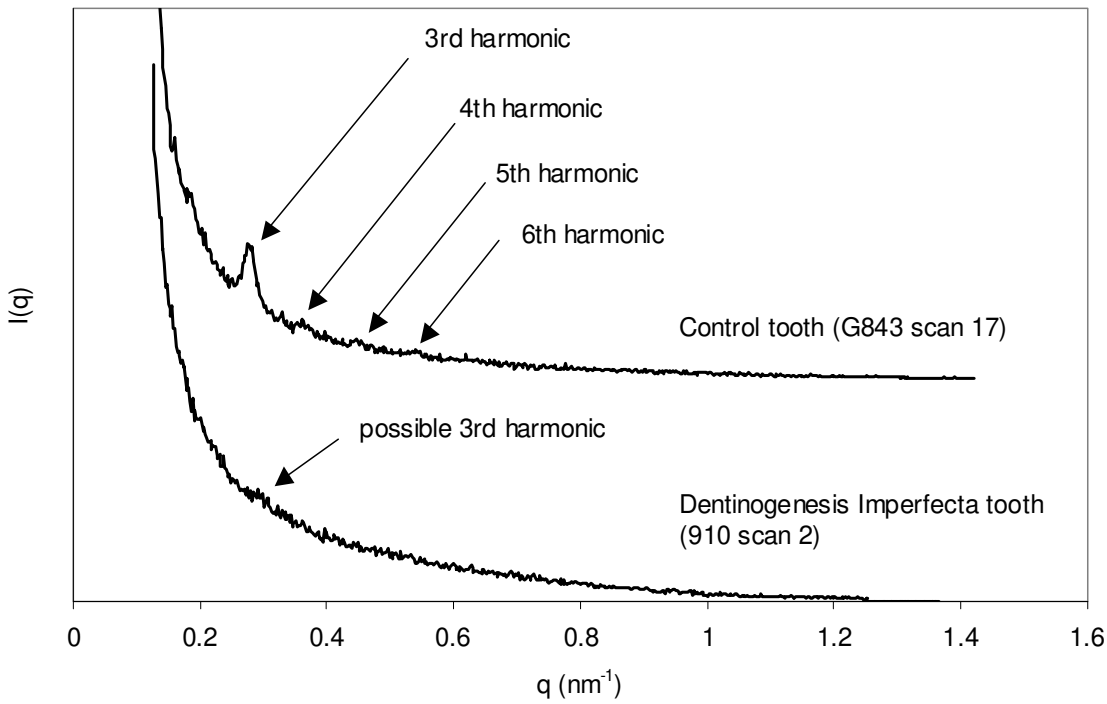

Figure 4: Small angle scattering patterns in normal (solid line) and DI-II (dashed line) dentin. The characteristic low-angle diffraction peaks in normal dentin, representative of intrafibrillar mineralization, were not as pronounced in DI-II dentin. Also, there was a measurable contraction in the separation of the intrafibrillar mineral in the DI-II dentin as compared with normal dentin.

DISCUSSION

Prior studies with the turkey-tendon model of biomineralization lend support to heterogeneous mineral nucleation both at the gap zones within the collagen fibrils (intrafibrillar) as well as in the interstices separating the collagen fibrils (extrafibrillar) (Landis *et al.*, 1996b). The proportion of mineral in each site has not been firmly established, and may vary with tissue type and location. However, it is estimated that in normal bone the majority (upwards of 75%) of the mineral is extrafibrillar (Pidaparti *et al.*, 1996). Therefore, it is not unreasonable to expect a similar proportion of extrafibrillar mineral in dentin. It is also believed, based on high-resolution electron microscopy, that the intrafibrillar mineral is predominantly plate-like (Landis *et al.*, 1996a), while extrafibrillar mineral may be more needle-like in conformation (Bonucci, 2000), although this is still controversial.

Herold, in a TEM study of DI-II dentin from primary teeth, observed that the collagen fibrils were coarser and more irregularly organized than in normal dentin. (Herold, 1972). The periodic banding, due to the overlap zones in the fibrils, was still present. However, the gap zones appeared devoid of mineral; instead, most of the mineral appeared to lie outside the fibers in the interstitial space.

Our findings provide substantial supporting evidence that intrafibrillar mineralization may be absent in DI-II. First, the near absence of low-angle diffraction peaks in DI-II dentin suggested that the periodically spaced crystallites associated with intrafibrillar mineralization of the gap zones were not as common in DI-II dentin as in normal dentin. Second, the needle-like conformation of the mineral crystallites in DI-II

dentin was consistent with extrafibrillar mineralization. Third, the roughly 30% reduction in total mineral concentration from that of normal dentin was consistent with the estimates of 25-30% of the mineral in normal dentin being intrafibrillar.

The crystallite thickness was significantly greater in DI-II than normal dentin. It is possible that the intrafibrillar crystallites are thinner than the extrafibrillar; absence of the latter would increase the mean thickness of the remaining crystallites. We believe this is unlikely, however, because an earlier study showed the crystallite thickness was independent of shape, implying the average crystallite thickness was the same for both extra- and intrafibrillar locations in normal dentin (Kinney *et al.*, 2000b).

We believe it to be more likely that the crystallites in DI-II dentin are thicker as a result of the coarser, more irregularly organized collagen fibrils. The extrafibrillar space would be greater, perhaps relaxing geometric constraints on crystal growth. We should also mention that if intrafibrillar mineralization is absent in DI-II, then the noncollagenous proteins associated with this disease must primarily promote mineralization and binding to the collagen fibrils. Their effect on extrafibrillar mineralization, if any, must be secondary. More study of these possibilities is warranted.

The absence of intrafibrillar mineralization would be expected to have pronounced effects on the mechanical properties of the dentin. A hint of this was seen in the buckling of DI-II dentin with drying. In normal dentin, the presence of intrafibrillar mineralization would act to resist complete shrinking of the collagen fibrils with drying, thereby reducing the buckling stresses.(Kinney *et al.*, 1993) In the absence of this resistive reinforcement, the collagen fibrils would impose larger stresses on the dentin, producing the buckling seen in the DI-II dentin in this study. This possibility was supported by the contracted separation measured in the diffraction pattern of the DI-II dentin: 63 nm vs 67.6 nm in normal dentin.

This study was limited to the evaluation of several DI teeth from a single patient. Unfortunately, this has also been true of the vast majority of all studies of this disorder. Therefore, without further corroborative studies, it is inappropriate to generalize our findings to all patients with DI-II. However, the histological agreement with prior case studies, as well as the previous TEM observation that failed to find intrafibrillar mineral, suggest that the absence of intrafibrillar mineral in DI-II must be considered a real possibility. More study is warranted.

In summary, our measurements of mineral density and the small angle scattering patterns are consistent with an absence of intrafibrillar mineral in DI-II. If there is a great reduction, or absence of intrafibrillar mineralization in DI-II dentin, then this disease might provide a unique opportunity to study the importance of the mineral-collagen interaction on mechanical and physiological function. It might also afford the opportunity to study the importance of noncollagenous proteins in biomineralization (Takagi *et al.*, 1983; Veis, 1989). This knowledge will be important for developing bioengineering approaches for conservative and restorative dentistry.

ACKNOWLEDGMENTS

The National Institutes of Health, National Institute of Dental and Craniofacial Research, supported this work through grant number P01 DE09859. We also acknowledge the support of the Stanford Synchrotron Radiation Laboratory (SSRL), U.S. Department of Energy, supported by DOE contract DE-AC03-76SF00515. We acknowledge the contributions of D.L Haupt for specimen preparation and G. Nonomura for maintaining the documented tooth collection from which these specimens were selected.

APPENDIX

The two dimensional scattering intensities, $I(x,y)$, were converted to polar coordinates, $I(q,\phi)$, where ϕ was the azimuthal scattering angle, and q was the wavevector given by:

$$q = \left(\frac{4\pi}{\lambda}\right)\sin\theta \qquad (1a)$$

Here, λ was the incident x-ray wavelength, and 2θ was the scattering angle. Following procedures described by Guinier (Guinier and Fournet, 1955), the azimuthally averaged scattering intensity can be described as a function of q:

$$I(q) = I_o T^3 F(qT)(1 + G(q)) \qquad (2a)$$

Here, the scattering form factor, $F(q,T)$, is a function of the shape of the crystallites, $G(q)$ is an interference function sensitive to correlations in the crystal positions, and T is a parameter related to the crystallite thickness.

The thickness parameter T, is related to the total surface area, S, and the total volume, V, of the mineral crystals:

$$T = \frac{4V}{S} \qquad (3a)$$

T was obtained from the scattering intensity at large q:

$$I(q) \xrightarrow{\approx} \frac{P}{q^4} \qquad (4a)$$

$$T = \frac{4}{\pi P}\int q^2 I(q)\,dq$$

The Porod constant, P, was determined by curve fitting the q^{-4} dependence of the scattering intensity at large q. Using the total scattering yield and the Porod constant P, the thickness parameter T was calculated directly from Equation 4. The thickness of the crystallites, τ, was estimated from the stereological relationship $\tau = T/2$.

REFERENCES

Aplin HM, Hirst KL, Dixon MJ (1999). Refinement of the dentinogenesis imperfecta type II locus to an interval of less than 2 centiMorgans at chromosome 4q21 and the creation of a yeast artificial chromosome contig of the critical region. *Journal of Dental Research* 78(6)*:*1270-6.

Bonucci E (2000). Basic composition and structure of bone. In: Mechanical Testing of Bone and the Bone-Implant Interface. YH An and RA Draughn editors. Boca Raton: CRC Press.

Fratzl P, Fratzl-Zelman N, Klaushofer K, Vogl G, Koller K (1991). Nucleation and growth of mineral crystals in bone studied by small-angle x-ray scattering. *Calcified Tissue International* 48(407-413.

Fratzl P, Groschner M, Vogl G, Plenk H, Eschberger J, Fratzl-Zelman N, Keller K, Klaushofer K (1992). Mineral crystals in calcified tissues: a comparative study by SAXS. *Journal of Bone and Mineral Research* 7(329-334.

Guinier A, Fournet G (1955). Small-Angle Scattering of X-rays. New York: John Wiley and Sons.

Herold RC (1972). Fine structure of tooth dentine in human dentinogenesis imperfecta. *Archives of Oral Biology* 17(6)*:*1009-13.

Kerebel B, Daculsi G, Menanteau J, Kerebel LM (1981). The inorganic phase in dentinogenesis imperfecta. *Journal of Dental Research* 60(9)*:*1655-60.

Kinney JH, Balooch M, Marshall GW, Marshall SJ (1993). Atomic-force microscopic study of dimensional changes in human dentine during drying. *Archives of Oral Biology* 38(11)*:*1003-7.

Kinney JH, Marshall GW, Jr., Marshall SJ (1994). Three-dimensional mapping of mineral densities in carious dentin: theory and method. *Scanning Microscopy* 8(2)*:*197-204; discussion 204-5.

Kinney JH, Haupt DL, Balooch M, Ladd AJC, Ryaby JT, Lane NE (2000a). Three-dimensional morphometry of the L6 vertebra in the ovariectomized rat model of osteoporosis: Biomechanical Implications. *Journal of Bone and Mineral Research* 15(1981-1991.

Kinney JH, Pople JA, Marshall GW, Marshall SJ (2000b). Collagen orientation and crystallite size in human dentin: A small angle x-ray scattering study. *Calcified Tissue International* in press(

Landis WJ, Hodgens KJ, Arena J, Song MJ, McEwen BF (1996a). Structural relations between collagen and mineral in bone as determined by high voltage electron microscopic tomography. *Microscopy Research and Technique* 33(2)*:*192-202.

Landis WJ, Hodgens KJ, Song MJ, Arena J, Kiyonaga S, Marko M, Owen C, McEwen BF (1996b). Mineralization of collagen may occur on fibril surfaces: evidence from conventional and high-voltage electron microscopy and three-

dimensional imaging. *Journal of Structural Biology* 117(1)*:*24-35.

Levin LS, Leaf SH, Jelmini RJ, Rose JJ, Rosenbaum KN (1983). Dentinogenesis imperfecta in the Brandywine isolate (DI type III): clinical, radiologic, and scanning electron microscopic studies of the dentition. *Oral Surg Oral Med Oral Pathol* 56(267-274.

MacDougall M, Gu TT, Simmons D (1996). Dentin matrix protein-1, a candidate gene for dentinogenesis imperfecta. *Connective Tissue Research* 35(1-4)*:*267-72.

Piattelli A (1992). Symmetrical pulp obliteration in mandibular first molars. *Journal of Endodontics* 18(10)*:*515-6.

Pidaparti RM, Chandran A, Takano Y, Turner CH (1996). Bone mineral lies mainly outside collagen fibrils: predictions of a composite model for osteonal bone. *Journal of Biomechanics* 29(7)*:*909-916.

Siar CH (1986). Quantitative histological analysis of the human coronal dentine in dentinogenesis imperfecta types I and II. *Archives of Oral Biology* 31(6)*:*387-90.

Takagi Y, Veis A, Sauk JJ (1983). Relation of mineralization defects in collagen matrices to noncollagenous protein components. Identification of a molecular defect in dentinogenesis imperfecta. *Clinical Orthopaedics and Related Research* 71(176)*:*282-90.

Thotakura SR, Mah T, Srinivasan R, Takagi Y, Veis A, George A (2000). The non-collagenous dentin matrix proteins are involved in dentinogenesis imperfecta type II (DGI-II). *Journal of Dental Research* 79(3)*:*835-9.

Veis A (1989). Studies of vertebrate tooth mineralization. Insights from studies of dentinogenesis imperfecta type II. *Northwestern Dental Research* 1(2)*:*3-5.

Waltimo J, Ranta H, Lukinmaa PL (1995). Ultrastructure of dentin matrix in heritable dentin defects. *Scanning Microscopy* 9(1)*:*185-97; discussion 197-8.

Wright JT, Gantt DG (1985). The ultrastructure of the dental tissues in dentinogenesis imperfecta in man. *Archives of Oral Biology* 30(2)*:*201-6.